GLOBAL ENGINEERS & TECHNOLOGISTS REVIEW
www.getview.org

THE FINITE ELEMENT ANALYSIS ON HEXAGONAL RING UNDER SIMPLE LATERAL LOADING

SAID[1], M.R., YUHAZRI[2], M.Y. and SAIJOD LAU[3]

[1]Faculty of Mechanical Engineering
[2]Faculty of Manufacturing Engineering
Universiti Teknikal Malaysia Melaka
Hang Tuah Jaya, 76100 Durian Tunggal, Melaka, MALAYSIA.
[1]radzai@utem.edu.my
[2]yuhazri@utem.edu.my

[3]Faculty of Engineering and Technology
Multimedia University
Jalan Ayer Keroh Lama, 75450, Melaka, MALAYSIA.
[3]twlau@mmu.edu.my

ABSTRACT

Lateral crushing of hexagonal ring under quasi-static loading were analysed using ABAQUS/Standard Finite Element (FE) Method package. The modes of deformation and load-displacement characteristics were predicted and the same were compared with experimental results. The material modelling of elastic-perfectly plastic and nominal stress-plastic strain were compared. The experimental results found that the quarter model using CPE6H with elastic-perfectly plastic material is good enough to obtain a satisfactory result.

Keywords: *Lateral Loading, Finite Element Analysis, Absorbing Mechanism.*

1.0 INTRODUCTION

Impact energy absorption (IEA) has been studied by many researchers. Recently Olabi *et al.* (2007) have reviewed IEA with respect to metallic tube. However, very recent paper reviewed by Saijod *et al.* (2012), on the composite material. There many types of IEA devices used, one them are a ring subjected to lateral loading. The energy absorption capacity of a ring under lateral compression was first addressed by Mutchler (1960). Two different kinematically admissible collapse mechanism that produce the same post-collapse load-deflection characteristic when employing a rigid perfectly-plastic material model were put forward by DeRuntz and Hodge (1963) and Burton and Craig (1963). Careful and exhaustive experiments on the crushing of tubes and rings done by Reddy and Reid (1980) led to the formation of a model that is based on the classical elastica theory that used a rigid linear strain hardening material behaviour, Reid and Reddy (1978). As a result of this analysis, load-deflection curves were seen in very good agreement with experimental observations. This analysis has since come to be known as “plastica" after being addressed by several authors starting with Yu and Johnson (1982).

Reddy and Reid (1979) examined the behaviour of laterally compressed tubes under transverse constraints and noticed that the collapse load increased by a factor approximately 2.4 and the energy absorbed increased by a factor of 3 in comparison with transversely unrestrained tubes. An excellent review of the energy absorbing systems, that use the lateral compression of metal tubes is given by Reid (1983, 1985).

Plastic collapse of square tubes compressed laterally between two plates was studied by Sinha and Chitkara (1982) who produced plastic collapse mechanisms. Gupta and Ray (1998) have performed experiments on this-walled empty and filled square tubes laterally compressed by using a rigid platen. They analysed the problem with the Sinha and Chitkara (1982) mechanisms and assumed plastic hinges occurred at only at mid section of vertical side, while in horizontal side to be elastic bending. These analyses used plastic hinges and could be modified by replacing plastic hinges with plastic zones (Reddy, 1978). Gupta and Sinha (1990) have studied the post-collapse behaviour of square tubes under transverse loads applied by flat short-width indenters as well as considering tubes compressed between an indenter and a rigid platen.

Johnson and Reid (1978) cited the energy absorbing devices with hexagonal shapes referring to an article of Fuse and Fukuda, 1973 (in Japanese) where in hexagonal tubes under quasi-static compression across faces were studied. The mechanism of collapse has hinges at the side corners and at the centres of loaded faces. Although the collapse load is in good agreement with experiment, the theory overestimates the post collapse loads. No alternatives collapse mechanisms appears to have been considered. The case of hexagonal ring loaded

across its diagonal has not been studied numerically so far. This paper presents the Finite Element Method to study the accuracy with experimental results done by Said and Reddy (2002).

2.0 MODELLING OF HEXAGONAL RINGS

Two material models were used for as-received material. First, the nominal stress-plastic strain data from the tensile test were used to describe the material. Secondly, the material was modelled as elastic-perfectly plastic. The results of the two materials were compared. For the annealed material, the nominal stress-plastic strain data from tensile tests were used to adequately model the strain hardening effects. The stress-strain data used are graphically shown in Figure 1.

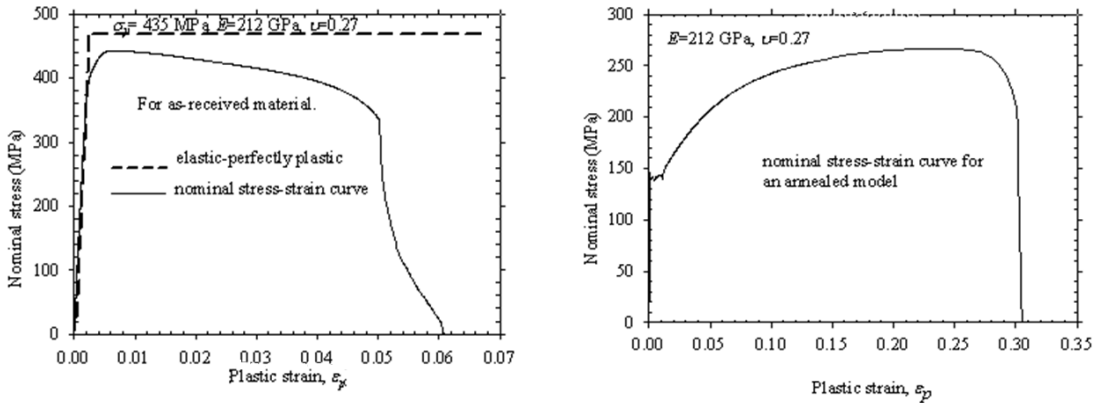

(a) **(b)**

Figure 1: Material properties used in ABAQUS analyses model **(a)** As-received material, **(b)** Annealed material.

Taking advantage of symmetry about two axes, only one quarter of the ring was modelled. Simple and side constraints lateral compression were examined for both across faces and corners loading. However, in this paper, simple lateral compression is only considered. Typical geometry and element mesh for several cases are shown in Figure 2. The depth of the model considered was 10 mm and thickness was 1.87 mm. The case of ground corners in solid elements model (Figure 2b) were also examined. Beam elements with quarter, half and full ring model were also used in the case of loading across faces to study the accuracy of ABAQUS/Standard Finite Element code.

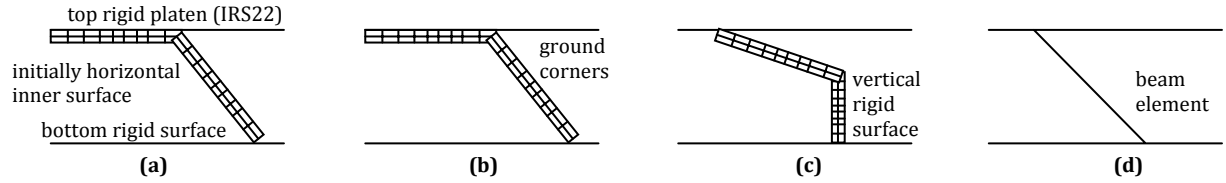

Figure 2: Typical geometry and mesh of quasi-static analysis using ABAQUS with solid and beam elements **(a)** non-ground corners model compressed across faces, **(b)** ground corner model compressed across faces, **(c)** ground corners model, side constraints and compresses across faces, **(d)** beam element model compressed across faces.

2.1 Solid Elements.

Forty eight six-noded elements (CPE6H), quadratic plane strain triangle and hybrid made up a quadrant of the specimen without ground corners. It was found that typically a mesh consisting of 5 mm base by 0.935 mm height triangular element was good enough to accurately predict experimentally results. The typical mesh for non-ground and ground models is shown in Figures 2a and 2b, respectively for the case of simple compression across faces.

The model (with ground corner) for the case of simple compression across corners is shown in Figure 2c. The mesh and geometry used to model compression across faces was employed. A rigid surface element (IRS22) monitored the contact between the flat, horizontal rigid surface (top and bottom platen) and the specimen, in the case of simple compression (Figure 2a and 2b). The rigid platen was modelled as a rigid surface with the *RIGID SURFACE and located on the top model surface. *SURFACE DEFINITION option was used to define outer surface of model. The *CONTACT PAIR option then was used to model the contact between the outer surface and rigid platen. The inner surface of the specimen that came into contact with the central rigid platen (axis of symmetry) was defined by means of an interface element (IRS22) to avoid penetration. The effect of friction was considered by taking the coefficient of friction,μ as 0 and 0.3. Another element (CPE4H) was also used in the analysis for comparison with CPE6H.

In modelling the ground corners, the corner lines were chamfered to thickness, which was the same as side thickness. The typical mesh of ground corners model is shown in Figure 2b. The corner was modelled with smaller solid elements of CPE6H. The element size except at the corners was 5 mm base by 0.935 mm height. The total number of CPE6H elements and nodes were 65 and 207, respectively, which is shown in Figure 2b.

2.2 Beam Elements.

The B22 beam element used had a three-noded quadratic. Each side wall had 4 elements of 10 mm length, and hence there were 24 elements in the model of full hexagonal ring. A typical quarter model is shown in Figure 2d for loading across faces. As in the solid element, the rigid platen was modelled as *RIGID SURFACE, but its location was in mid-section of the hexagonal ring. This three noded quadratic beam element uses Timoshenko beam theory, which allows large strain deformation and includes transverse shear deformation.

3.0 RESULTS AND DISCUSSION

The load-displacement curves are shown in Figure 3(a) until Figure 3(h). The deforming meshes are shown in Figure 4 and Figure 5 (for solid elements) meanwhile in Figure 6 and Figure 7 is for beam elements.

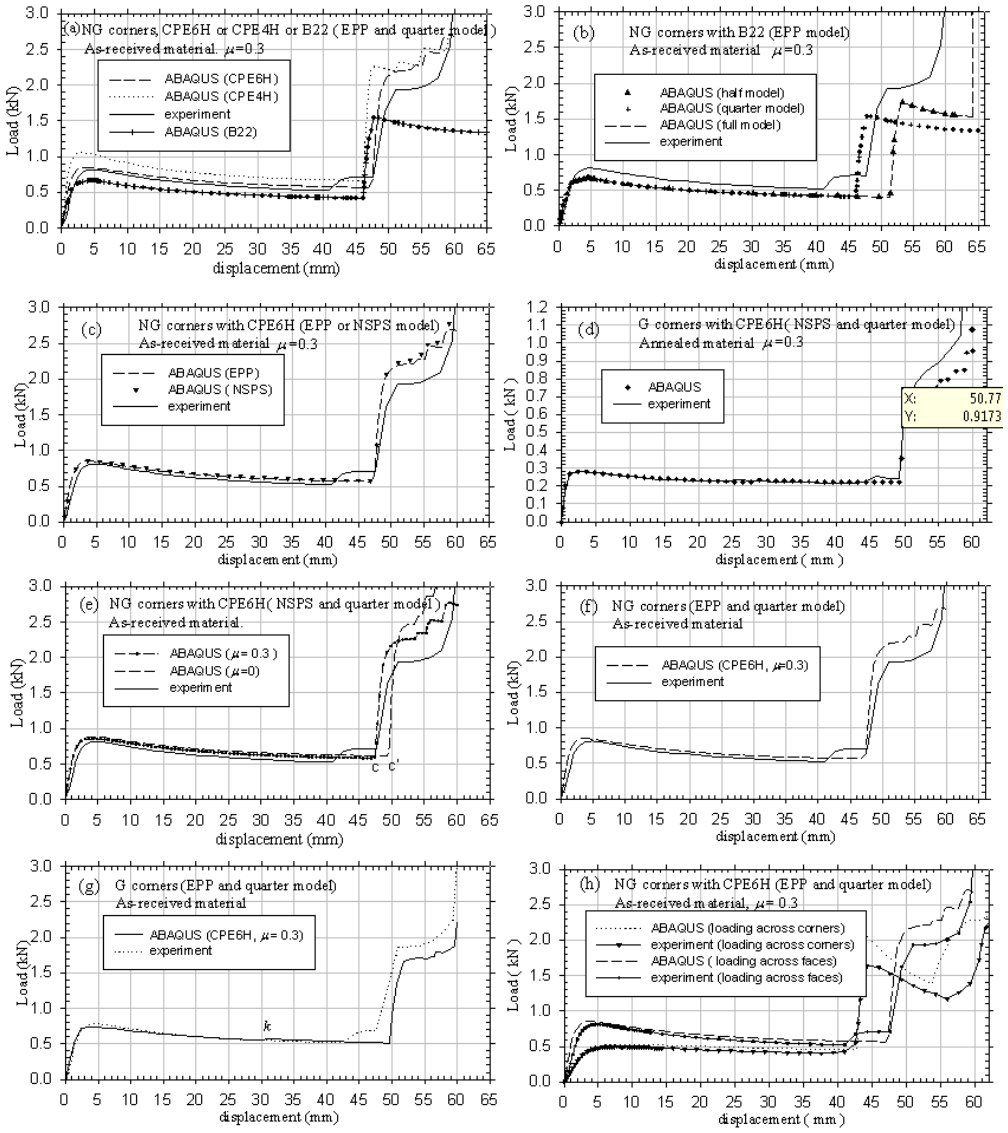

NOTE : EPP for elastic-perfectly plastic, NSPS - nominal stress-plastic strain, NG - non-ground and G- ground

Figure 3: Load-displacement curve of hexagonal rings laterally compressed across faces **(a)** Solid elements (CPE6H and CPE4H), beam element (B22) and experiment, **(b)** Quarter, half and full model, ABAQUS analysis with B22 element, **(c)** Elastic perfectly-plastic, nominal stress-plastic strain material model with ABAQUS and experiment, **(d)** ABAQUS (CPE6H) and experiment for annealed material, **(e)** ABAQUS (m=0 and m=0.3) and experiment, **(f)** ABAQUS (CPE6H) and experiment for NG corners, **(g)** ABAQUS (CPE6H) and experiment for G corners, **(h)** ABAQUS and experiment for loading across faces and across corners (b = 40 mm, t = 1.87 mm, and w = 10 mm).

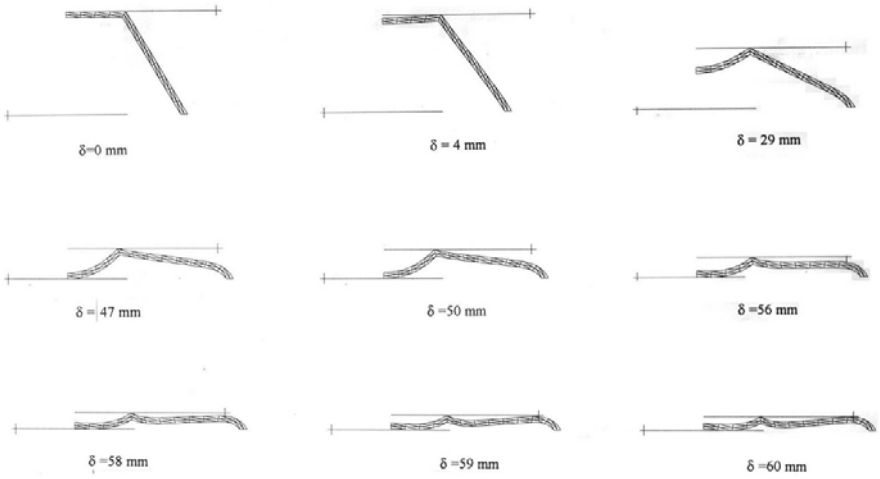

Figure 4: Deformation of a ring (non-ground corners) compressed across faces predicted by ABAQUS with solid elements (CPE6H) and elastic perfectly plastic material.Only quarter of the ring shown.

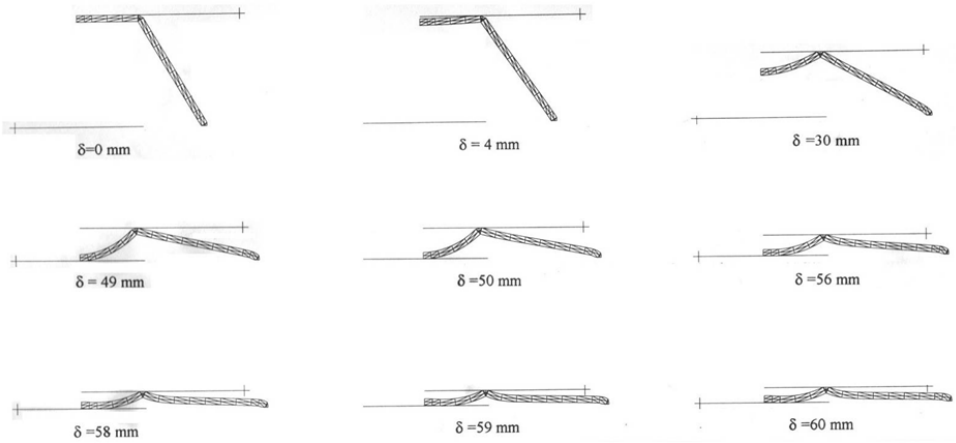

Figure 5: Deformation of a ring (ground corners) compressed across faces predicted by ABAQUS with solid elements (CPE6H) and elastic perfectly plastic material. Only quarter of the ring shown

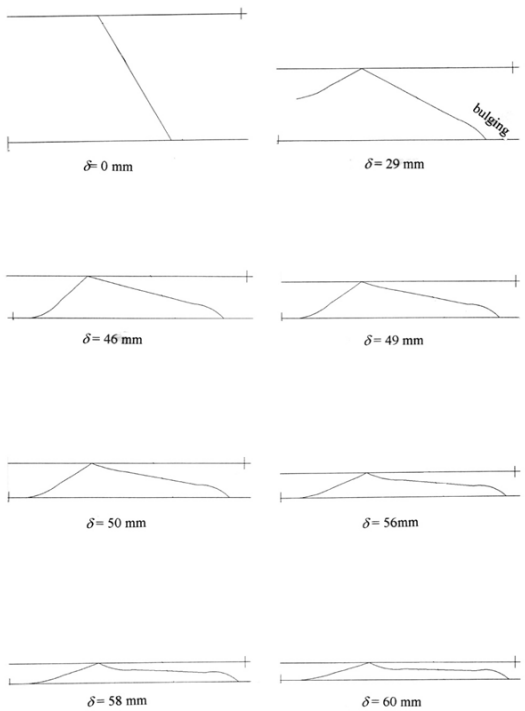

Figure 6: Deformation of a ring (ground corners) compressed across faces predicted by ABAQUS with beam elements (B22) and elastic perfectly plastic material. Only quarter of the ring shown

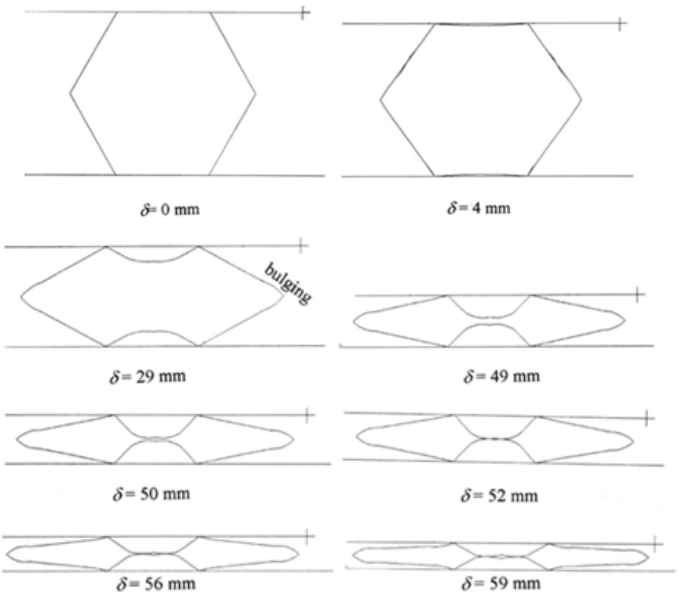

Figure 7: Deformation of a ring compressed across faces predicted by ABAQUS with beam elements (B22) and elastic perfectly plastic material. A full model of the ring shown

A summary of FEM results of rings compressed across faces is as presented in Table 1. The summary results include the collapse load, F_c displacement when the top and bottom ring faces touch, δ_{tb} and energy absorbed, W of experimental results.

Table 1: A summary of FEM results of lateral compression on hexagonal rings (simple lateral compression and side constraints compression). (model dimensions: b=40 mm, t=1.87 mm, w=10 mm)

Type of lateral loading	Element type, Ground or Non-ground corners and as-received or annealed.	*EPP or NSPS model and coefficient of friction		Collapse load, F_c (kN)	Displace-ment, *δ_{tb} (mm)	Energy absorbed,W at δ_{tb} (Nm)
Simple lateral compression across faces	CPE6H, Non-ground corners, (as-received)	NSPS	μ =0	0.88	49	34.4
			μ =0.3	0.86	47	31.4
		EPP(μ =0.3)		0.85	47	31.2
		Experiment(H1)		0.83	48	29.8
	CPE6H, Ground corners, (as-received)	EPP (μ =0.3)		0.74	50	29.2
		Experiment(H1)		0.8	46	28.4
	CPE6H, Non-ground corners, (annealed)	NSPS (μ =0.3)		0.28	49	11.6
		Experiment(H1)		0.28	49	8.63
	CPE4H, Non-ground, (as-received)	EPP (μ =0.3)		1.06	46	36
	B22 (as-received)	EPP (μ =0.3)	quarter	0.7	46	23
			half	0.67	51	25.2
			full	0.67	51	25.2

NOTE : *EPP-elastic perfectly plastic, NSPS-nominal stress-plastic strain, H1-compression at 20 mm/min
δ_{tb}- displacement when specimen model in contact with bottom rigid platen contact.

Four parameters are discussed in this section to check the accuracy of FEM. Those are geometric modelling, material modelling, friction and corner grinding effect

(i) Geometric modelling.

a) Solid element CPE6H, CPE4H and beam elements (B22).

Figure 3(a) illustrates a comparison of experiment with the load-displacement curves produced by the FEA using solid elements (CPE6H and CPE4H) and beam elements (B22). In all cases, non-ground corners

and quarter models were used. A coefficient of friction, 0.3 was used and the material was assumed to be elastic-perfectly plastic. It is seen that the curve produced with six noded, quadratic, triangular plane strain hybrid pressure elements (type CPE6H) is in close agreement with the experiment, the difference <10%. Bending in elements is dominant in the CPE6H quadratic element, which is important in the present deformation process. This can also be seen in deforming mesh shown in Figure 4a-b. This is not the case with the CPE4H model. As a result, load-displacement curve predicted by CPE4H elements overestimates the experiment by about >30% at collapse (Figure 3a) and the difference gradually decreases to about 10% when central sections of the ring come into contact with each other. This may be due to the fact that no bending effects are allowed in the bilinear element CPE4H, thus enhancing the load. The agreement may be closer with a finer element mesh. On the other hand, beam element (B22) underestimates the experimental results by ranging from about 20% at collapse and 40% at the onset of contact. This may be also due to fact that, the beam element is one dimensional and the variables (such as stresses, strains) are functions of position along the beam axis only.

b) Quarter, half and full models with beam elements.

Figure 3b shows the load-displacement curves obtained using quarter, half and full ring models employing beam element (B22) in the ABAQUS package using an elastic-perfectly plastic material model for all cases. All the models produce identical characteristics except that the inner upper part come into contact with rigid body in the quarter model at a displacement of 23 mm (total 46 mm) and with the inner lower part in case of half and full ring models, at a displacement of 52 mm. The deformation patterns produced by the quarter and full model analyses are shown in Figure 6 and Figure 7. A 'bulging' begin to form at the side corners at a displacement of 29 mm in all three cases, it continues until the model is completely crushed. The reason for this 'bulging' is not clear and is not explored. The half and full ring models produced identical behaviours throughout the displacement regime. This analysis indicates that the quarter ring model is good enough to obtain results that agrees well enough with the experiment.

(ii) Material modelling.

a) Elastic-perfectly plastic and nominal stress-plastic strain curve for as-received material.

Figure 3c shows the two load-displacement curves predicted using the two material models, i.e. elastic-perfectly plastic and nominal stress-plastic strain curve for the case of as-received material along with the experimental characteristic. The analysis was carried out using solid elements (CPE6H) and non-ground corners with μ =0.3. The predictions of the two material models are identical. Table 1 shows that the collapse load and energy absorbed are the same for both cases. Hence, it may be inferred that the elastic-perfectly plastic model produces results as accurate as the nominal stress- plastic strain curve for the as-received material. This is also good enough to predict the experimental result by using elastic-perfectly plastic model. However, the differences between prediction and observation in the elastic region are slightly higher than in the post collapse regime. This might be due to small curvatures at corners and any non-uniformities in thickness in the experimental specimen The deformed shapes predicted with the elastic-perfectly plastic material model are plotted in Figure 4.

b) A nominal stress-plastic strain curve for annealed material.

Figure 3d shows the predictions using nominal stress-strain curve for an annealed mild steel ring along with the experimental characteristics. The analysis used CPE6H solid element and non-ground corners in the model with μ =0.3. The numerical load-displacement characteristic shows close agreement with the experimental results. The collapse load, F_c and displacement, δ_{tb} where the load begins to steeply increase, for both cases are the same, which is about 0.28 kN and 49 mm, respectively (row 3 in Table 1). There are also no significant differences in the predicted and observed deforming patterns.

(iii) Frictional effects.

The FE model used CPE6H element and non-ground corner case. Nominal stress-plastic strain curve was used for the as-received material of the ring. Figure 3e shows the of load-displacement curves with coefficient of friction values of 0 and 0.3 and indicates that friction has negligible effect on the collapse load and has marginal effect (maximum of 5%) on the post collapse loads. However, in the frictionless model, the inner central faces come into contact at a displacement of 47 mm, 2 mm smaller than that when friction is included. These are shown as points c and c' in Figure 3e.

(iv) Influence of corner grinding.

Figure 3f and Figure 3g illustrate the load-displacement curves for rings with non-ground and ground corners crushed across the faces. CPE6H elements with μ =0.3 are used in the FE analysis, which is compared with experimental results. The slope of the elastic line in load-displacement curve for ground corners model is closer to the experiment curve, as seen in Figure 3g. There was a slight blip that appears in the case of ground corners (at about 30 mm displacement) on curve at '*k*'**,** as the rigid platen came into contact with the chamfered surface. The deforming mesh at this instant is shown in Figure 5 at δ=30mm.

The inner mid face came into contact with the bottom rigid surface at a displacement of 50 mm in ground case, while in non-ground case this was at 47 mm (Figure 3f and Table 1). The deforming meshes at these displacements are shown in Figure 4 and Figure 5. In general, the load-displacement curve for non-ground model is slightly higher by a maximum of approximately 10% compared with experimental curve while for ground cases, they are in close agreement.

4.0 CONCLUSION

Experiment suggests that the elastic-perfectly plastic model produces results as accurate as the nominal stress-plastic strain curve for the as received material and the quarter ring model is good enough to obtain a satisfactory result. It shows that solid element, CPE6H produced the best results. The friction has negligible effect on the collapse load and has marginal effect on the post collapse loads.

REFERENCES

[1] Burton, R.H. and Craig, J.M. (1963): An Investigation Into The Energy Absorbing Properties Of Metal Tubes Loaded In The Transverse Direction. Thesis for B.Sc., University of Bristol.

[2] DeRuntz, J.A. and Hodge, P.G. (1963): Crushing of a Tube between Rigid Plates. *J.Appl. Mech.*, vol.30, pp.391-395.

[3] Fuse, H. and Fukuda, H. (1973): Plastic Deformation Characteristics Of Polygonal Cross Section Cylinders. Meiji University Department of Engineering, Report No. 26-27, I-62, 31.

[3] Gupta, N.K. and Sinha, S.K. (1990): Collapse of a Laterally Compressed Square Tube Resting On a Flat Base. *Int. J. Solid Structure*, vol.26, no.5/6, pp.601-615.

[4] Gupta, N.K. and Ray, P. (1998): Collapse of Thin-Walled Empty And Filled Square Tubes Under Lateral Loading Between Rigid Plates. *International Journal of Crashworthiness*, Vol.3, No.3, pp.265-285.

[5] Johnson, W. and Reid, S.R. (1978): Metallic Energy Dissipating Systems. *Applied Mechanics Reviews*, vol.31, No.3, pp.277-288.

[6] Mutchler, L.D. (1960): Energy Absorption in Aluminium Tubing. *J.Applied Mech.*, vol.27, pp.740-743.

[7] Olabi, A.G., Morris, E. and Hashmi, M.S.J. (2007): Metallic Tube Type Energy Absorbers: A Synopsis. *Thin-walled structure,* vol.45, pp.706-726.

[8] Reddy, T.Y. and Reid, S.R. (1980): Phenomena Associated With the Crushing Of Metal Tubes between Rigid Plates, *International Journal of Solids and Structures,* vol.16, p.545.

[9] Reddy, T.Y. and Reid, S.R. (1979): Lateral Compression of Tubes and Tube-Systems with Side Constraints. *Int. J of Mech. Sci.,* vol.21, p.187.

[10] Reddy, T.Y. (1978): Impact Energy Absorption Using Laterally Compressed Metal Tubes. Thesis for PhD, Department of Engineering, University of Cambridge, England.

[11] Reid, S.R. (1983): Laterally Compressed Metal Tubes As Impact Energy Absorber. in *Structural Crashworthiness* (ed) Jones, N. and Wierzbicki, T. (Butterworth),pp.1-43.

[12] Reid, S.R. (1985): Metal Tubes as Impact Absorbers. in *Metal Forming and Impact Mechanics* (ed) Reid, S.R. (Pergamon Press), Chapter 14, pp.249-269.

[13] Reid, S.R. and Reddy, T.Y. (1978): Effect of Strain Hardening on the Lateral Compression of Tubes between Rigid Plates. *Int. J. Solid and Structures*, Vol.14, pp.213-225.

[14] Said, M.R. and Reddy, T.Y. (2002): Quasi-Static Response Of Laterally Simple Compressed Hexagonal Rings. *Int. Journal Crashworthiness,* vol.7, No.3, pp.345-363.

[15] Sinha, D.K. and Chitkara, N.R. (1982): Plastic Collapse of Square Rings. *Int. J. Solid. Structure.*, vol.18, no.18, pp.819-826.

[16] Wiesław, B., Pawel, D., Tadeusz, N. and Robert, P. (2011): Application of Composites to Impact Energy Absorption. *Computational Materials Science,* vol.50, pp.1233-1237.

[17] Yu, T.X. and Johnson, W. (1982): The Plastica: The Large Elastic-Plastic Deflection of A Cantilever. *Acta Linear Mech.* vol.17, pp.195-209.